Building and Environment 287 (2026) 113866

Contents lists available at ScienceDirect

Building and Environment

journal homepage: www.elsevier.com/locate/buildenv

Are we overestimating radiant effects? Re-examining view factors in the seated posture

Nour Youssef *, Katherine D'Avignon

École de Technologie Supérieure, Montreal, QC, Canada

ARTICLE INFO

Keywords:
Radiant heat exchange
View factors
Mean radiant temperature
Seated posture
Children
Thermal comfort
Radiant systems

ABSTRACT

Radiant heat exchange plays a critical role in occupant thermal comfort, and can be leveraged to increase building energy efficiency through radiant heating and/or cooling systems and personal comfort systems, for example. However, the view factors and projected area factors f_p of seated occupants, necessary for the adequate design of these systems, remain underexplored and often rely on outdated assumptions. This study investigates the impact of two long-standing simplifications—anterior-posterior (A/P) symmetry and the neglect of seat shading—on radiation data for both adult and child occupants in the seated posture. Using numerical manikins in various seated configurations (floating, on a stool, and on a chair), f_p values are calculated and tabulated, and their influence on view factors and mean radiant temperature is assessed. Results indicate that the A/P symmetry assumption holds only where no seat is present (as if the occupant were floating), and seat shading significantly reduces radiant exposure—up to 86 % for an adult in an office chair. Comparisons between adult and child manikins reveal minimal differences (<12 %) in the seated posture, suggesting that age-specific radiation data may be less critical for seated children than previously found for standing postures. Two test cases demonstrate that using standard view factors relying on these assumptions overestimates $\bar{t}_r$ by up to 2 °C, which could compromise occupant thermal comfort. These findings call for updated design and evaluation practices to account for seat shading effects in indoor spaces where occupants remain in the seated posture for prolonged periods.

1. Introduction

The determination of view factors F and projected area factors f_p is an important endeavour in thermal comfort literature due to the significant role of radiation in occupant comfort in both indoor and outdoor environments [1,2]. Outdoors, research shows that radiation from the ground can increase the risk of heat stress [3–5]. In the indoor environment, radiant heated floors and chilled ceilings have gained traction due to their superior performance in both delivering thermal comfort with reduced energy consumption [6,7], increasing their deployment in office and institutional buildings [8–10]. Yet, the effect of radiation on occupant comfort is still evaluated from data determined in long-dating experiments which few have been able to replicate, and relied on assumptions which have never been verified.

Humans spend 90 % of their time indoors [11] and 40–55 % of that time sitting down [12]. Though research on occupant radiation in the standing posture has expanded from the early methods and populations studied [13–15], very little literature can be found on the seated posture. This paper seeks to address these lacunas by determining the radiation data of an adult and child numerical manikin in the seated posture under various scenarios, addressing several of the calculation assumptions held in the literature.

2. Literature review

When an occupant is in a moderate indoor environment, ASHRAE-55 recommends the calculation of the Mean Radiant Temperature $\bar{t}_r$ using Eq. (1). In those circumstances, the dominant form of radiation present is the long wave emissions of the surrounding surfaces, which are assumed to be grey, diffuse, isothermal, and at a low temperature so view factors are used. $\bar{t}_r$ is defined as the uniform temperature of a hypothetical black-body enclosure that would produce the same net radiative heat exchange with the subject as the actual, more complex radiative environment, t_i is the temperature of each surrounding surface, and $F_{p\rightarrow i}$ is the view factor between the occupant and that surface [16]. On the other hand, direct solar-beam radiation can be characterized by a

* Corresponding author at: École de technologie supérieure, Montreal, Quebec Canada.
E-mail address: nour.youssef.1@ens.etsmtl.ca (N. Youssef).

https://doi.org/10.1016/j.buildenv.2025.113866
Received 5 August 2025; Received in revised form 22 September 2025; Accepted 14 October 2025
Available online 14 October 2025

small area, high temperature, and high directional radiant emission at a large distance, so the projected area factor f_p is used for the calculation of solar radiation effects on occupants. Therefore, knowledge of f_p and $\overline{t_r}$ enables us to derive an expression of the total net thermal radiation leaving the body R, as shown in Eq. (2), expressed as the difference between the long-wave emission of the body R_{lw} and absorbed short-wave radiation from the sun R_{sw}. σ is the Stefan-Boltzmann constant, ε is the emissivity of the human body, α_{ir} is the absorptivity of the skin/clothing for the short-wave band considered (in this case the sun), A_{eff} is the effective radiation area of the human body in m^2, and q_{ir} is the intensity of radiation emitted by the sun in watts.

$$\overline{t_r} = \sqrt[4]{\sum_{i=1}^{N} t_i^4 F_{p\to i}} \tag{1}$$

$$R = R_{lw} - R_{sw} = \sigma\varepsilon A_{eff}\left[t_{cl}^4 - \overline{t_r}^4\right] - \alpha_{ir} f_p A_{eff} q_{ir} \tag{2}$$

The view factor F is a mathematical geometrical property that depends on the location of the occupant (i.e. their distance and orientation from surrounding surfaces), the size of the considered surface (variables a, b, and c in Fig. 1), as well as the occupant's posture, meaning view factors are different for seated and standing persons. The projected area factor f_p is dependent on the orientation of the radiating surface with respect to the person, as expressed through the azimuth and altitude of the surface with respect to the occupant (variables α and β in Fig. 1), as well as the occupant's posture. Despite the presence of other measurement tools for the assessment of the mean radiant temperature, calculation through view factors remains the most reliable method [17,18].

Fanger [19] provides diagrams illustrating view factors for a nominal occupant in either the standing or seated posture with various rectangular surfaces in its surrounding for the purpose of direct mean radiant temperature calculations. Computer codes have recently been developed [16,20,21] that instead determine F for a specific surface using Fanger's f_p arrays in Eq. (3). Therefore, f_p is the single parameter needed to determine the total radiant exchange of the occupant with his environment, taking into account both the long-wave R_{lw} and short-wave R_{sw} component of that exchange.

$$F_{P-A} = \frac{1}{\pi}\int_{\frac{x}{y}=0}^{\frac{x}{y}=\frac{a}{c}}\int_{\frac{z}{y}=0}^{\frac{z}{y}=\frac{b}{c}} \frac{f_p}{\left[1+\left(\frac{x}{y}\right)^2+\left(\frac{z}{y}\right)^2\right]^{3/2}} d\left(\frac{x}{y}\right) d\left(\frac{z}{y}\right) \tag{3}$$

The values of F and f_p provided by standards [16,22,23] and used by professionals [21] are those extracted from the Fanger study [19] where adult participants were photographed in the standing and seated posture using an orthographic projection camera rotated front to back ($0° \le \alpha \le 180°$ on Fig. 1) and front to top ($0° \le \beta \le 90°$) in fifteen-degree

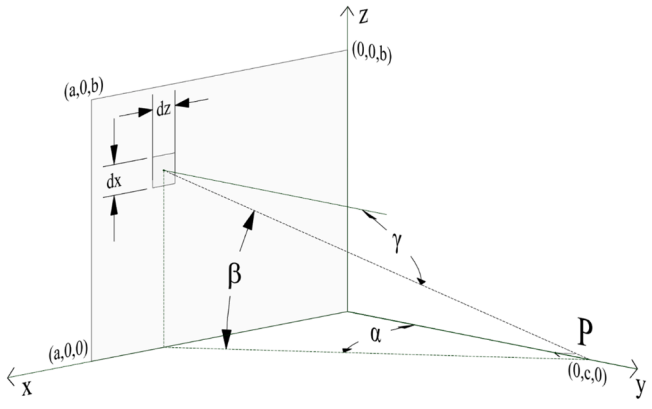

Fig. 1. Diagram of the basis for the evaluation of the view factor between a person (P) and a rectangular surface, reproduced from [19].

increments. Only one fourth of the sphere was considered, as left-right L/R and anterior-posterior A/P symmetry was assumed. As shown in Fig. 2a, L/R refers to vertical axis symmetry of the left and right side of the human body, so a person's f_p at the same angle β from their left side and right side (meaning at (α,β) and (-α, β)) are presumed equal. Literature has demonstrated this to be a reasonable assumption in healthy non-disabled adults and children [24] provided pose is also symmetrical across the vertical axis. A/P symmetry refers to the point symmetry of the front and back side of the human body with respect to the centre of volume, where a surface that is in front of and above the occupant's centre of volume is assumed to have the same f_p as that of a surface behind and below, as shown in Fig. 2b This assumption is illustrated in Fanger's cases one to six [19]. Following this assumption, the f_p values for surfaces that are below the occupant's center of volume were never measured in Fanger's experiments, but were instead determined through Eq. (4) [21].

$$if\ \beta < 0 \Rightarrow f_p(\alpha,\beta) = f_p(180-\alpha,-\beta) \tag{4}$$

Using such f_p for the calculation of F between the occupant and the floor is only applicable if no objects intercept the line of sight between the two. For the seated posture, the object upon which the occupant sits would effectively shade parts of the occupant's body from certain sections of the floor. Knowing Fanger's participants were most likely seated on a stool during his experiments; this would have affected the projected areas photographed for values of $\alpha > 90°$ (i.e. shading the back of the occupant's legs). The most significant shading effect of the seat would only be appreciated for negative values of β, which were not considered in the Fanger experiment. Other studies that used Fanger's data (whether his f_p arrays or his F diagrams), either to reproduce them using a numerical algorithm [25,26] or to expand their applicability to complex room shapes [27], inherently make those same assumptions.

Horikoshi et al. [14] conducted a study using the photographic method with four adult male subjects. They set themselves apart from the Fanger study by taking photographs at close distances from the subjects: 1 and 2 m They hypothesized the large distance between subject and camera in Fanger's work (7 m) made their data inapplicable to calculations where surfaces are at a close distance from occupants, such as floors. In addition, they did not assume A/P symmetry and determined F (but not f_p) for floor surfaces. In the seated posture, their findings were largely different from Fanger's, reaching a 40 % difference in F for the floor. The study did not describe nor address the presence of any seat in the experiment, nor the shading ensued. Instead, they concluded differing results were born out of the distinct photographic methods used, which would be exacerbated at short distances. A recent numerical investigation that replicated Horikoshi's experiment at close distances found differing results and posited that this discrepancy was born out of methodological issues in Horikoshi's work [28].

La Gennusa et al. [29,30] and Calvino et al. [31] conducted experimental studies on subjects representative of the southern Italian population, based on the method proposed by Calvino et al. [32]. In the original photographic experiment of [32], occupants were seated on a backless chair (i.e. a stool) which researchers stated strongly interfered with the visibility of the subjects' legs. They considered this interference to be unwanted, and so the images were "treated" to eliminate the stool from the photographs. None of these studies discussed the shading effect of the chair in possibly reducing the real radiant exchange of the body with the floor. All three studies determined f_p from the same altitude angles used by Fanger, effectively assuming A/P symmetry.

Lo Cursio [33], as reported by Nucara et al. [34], determined f_p numerically using adult numerical manikins of men and women both in the standing and seated postures. In the seated posture, the study claims a "significant agreement" with Fanger's data, except at $\beta = 30°$ where the difference reached 0.08 (45 %). The study also assumed A/P symmetry, opting to only determine f_p for positive values of β. They did not model a seat, and the effect of seat shading was not discussed.

Tanabe et al. [35] and Kubaha et al. [36] used floating seated

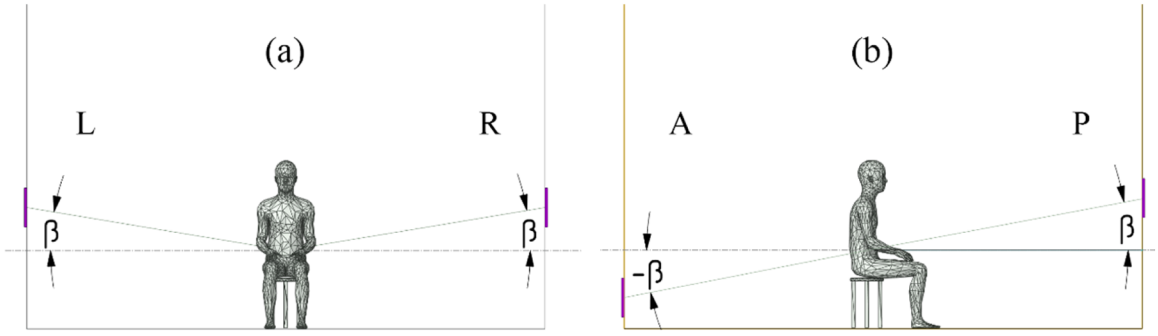

Fig. 2. Illustrations of the (a) Left/Right (L/R) symmetry as seen from $\alpha = 0°$, and (b) Anterior/Posterior (A/P) symmetry as seen from $\alpha = 90°$.

numerical manikins and compared their f_p results to Fanger's. Despite both having found a good match when comparing their results in the standing posture, Tanabe found some discrepancy for the seated posture. Vorre et al. [37] determined the F of a floating manikin, using a ray tracing method in ANSYS CFD, and found a good match with those determined using Fanger's F diagrams. The absence of a chair was noted as a limitation by the authors.

Overall, A/P symmetry is a widely used assumption in view factor literature, and consequently most studies opt to only determined f_p for positive values of β. Despite several researchers noting the large effect seat shading should have on this data, seats are rarely modelled in numerical studies, and the effect of seat shading on the photographs taken is rarely addressed in experimental studies.

Some studies have focussed on the shading caused by furniture and/or other occupants. Manabe et al. [38] studied the effect of room occupancy density on F of seated manikins due to shading by other occupants. They did not discuss the effect of seat shading and modelled their manikins "floating" in the air with no seats beneath them. The study notes F found between the seated occupant and the floor surpassed that of the standing occupant, without making note of the unrealistic floating configuration. In all the cases considered, the view factor between the studied occupant and other occupants increases as occupant intensity increases, reaching a maximum of 0.27 in the seated posture when surrounded by 49 occupants. In all cases, the reported full body view factor with the floor is the highest due to the unrealistic "floating" configuration. Other studies acknowledged the effect of seat shading without treating the data accordingly [39,40]. Only Francisco et al. [41] determined the view factors between a simplified human manikin and surrounding surfaces that included a small seat, table, drawer unit, computer and screen. They found F between occupant and chair to be the highest ($F_{chair} = 0.08$) out of all the surrounding furniture, indicating the importance of shading by this specific piece of furniture. As a result, F found between the occupant and floor was much smaller ($\Delta F = 0.111$) than in Vorre's study which considered occupants to be floating [37]. These findings indicate the magnitude of the effect of shading from surrounding objects (seats, desks, tables, other occupants, etc.) is highly contextual. For the seated posture however, a seat of some form will indubitably be present, raising the question as to whether it may be wiser to systematically include minimal shading from a stool, than to generalize the use of view factors which neglect it altogether.

Fanger's data (both f_p and F) are used by standards such as ASHRAE-55 [16], ISO 7730 [23], and ISO 7726 [42] for the calculation of $\overline{t_r}$ for any occupants regardless of their anthropomorphic characteristics. Several researchers have sought to confirm whether the radiation data obtained by Fanger for young Scandinavian adult males, applies to other populations. Nucara et al. [34] reports that Lo Cursio [33] studied adult models of men and women with anthropometric data characteristic of different nationalities (Italian, Australian and British, Chinese, Japanese, German, and American) and found absolute differences in f_p ($\Delta f_p < \pm 0.017$ for standing and $\Delta f_p < \pm 0.018$ for seated) between the populations considered in both the standing and seated cases. Similarly, Calvino et al. [31] considered the southern Italian population and found differences in f_p of up to ±0.018 (8 %) in the standing posture, and up to 0.081 (52 %) in the seated posture when comparing to Fanger's Scandinavian subjects. Rykaczewski et al. [13] investigated the impact of BMI and height variations among the American adult population on their f_p and f_{eff} in the standing posture and found that differences <10 %, apart from extreme cases (BMI > 80th percentile) where Δf_p reached 42 %. Similarly, Tanabe et al. [35] found differences of 7 % in f_p when comparing a "standard" to a "10 % wider" adult male manikin. Park & Tuller [43] compared a normal- and over-weight Canadian adult men and women in the standing and walking postures and found absolute differences in $f_p < 0.017$. Children on the other hand, constitute a larger proportion of every population [44] and have larger anthropometric and body surface area differences from adults than differences found amongst adults [45], and recent investigations indicate adult radiation data does not always apply to them [12,28]. Youssef & D'Avignon [12] found a difference in f_p reaching 23 % and 0.036 when comparing a 5-y. o. child manikin in the standing posture to an adult. As the standing child's F with the floor was found to bear the greatest difference to the adult's F (up to 23 %), an investigation into the underestimation of floor F for children in the seated posture appears warranted.

Across human view factor literature, the general method used to quantify differences in radiation data stemming from one's methodological approach relies on comparing results to established literature, mainly the experimental results of Fanger. Thus, a manikin or sample of participants resembling the average anthropometric characteristics of participants in the Fanger study are used, their f_p or F are determined and compared to Fanger's resulting f_p or F values. Comparison of f_p curve shapes [13,31,35,36], relative and absolute differences [13,36,43,46], as well as regression models [35] are the most common methods used. The significance of differences found across different populations can then be judge relative to differences due to the methodological approach employed [43].

This paper aims to make a thorough investigation of radiation data for seated occupants. First, the effect of long-held assumptions for this posture, particularly anterior-posterior symmetry and the disregard for the effect of seat shading, on F and f_p are investigated. Then, the particularity of child occupants is examined for the seated posture. Finally, a test case is used to evaluate the influence of these assumptions on view factors in a sample room under two scenarios, one employing radiant floor heating and one employing a chilled ceiling.

3. Methodology

The approach used in this study is inspired by the method outlined in [12], which was used to determine radiation data for occupants in the standing posture. Numerical models for two seated adults and one seated child were created using the UMTRI human body shape generator [47] and parameters listed in Table 1. Anthropometric characteristics of the male manikin, "Youssef", represent the average of the 10 men in

Table 1
Anthropometric data of numerical manikins.

Manikin	Age [years]	Gender	Height [m]	BMI	SHS
Youssef	22	Male	1.78	22	0.51
Nour	22	Female	1.66	22	0.53
Adam	5	Male	1.125	16	0.53

Fanger's 1970 study [19], while the female manikin, "Nour", is based on the mean of the 10 women in said study. As the sitting-height-to-stature (SHS) ratio of the subjects was not specified in the original work, average SHS data for northern European young adult men and women [48] were used, as shown in Table 1. The child manikin, "Adam", was created based on the anthropometric characteristics of the 50th percentile 5 y.o. American boy from the CDC [45].

The manikin postures produced by the UMTRI generator are typical of car seat occupants (i.e., inclined seatback, inclined seat cushion, raised arms, etc.) and were adjusted in Blender [49] towards more typical postures associated with indoor seating: manikins were adjusted so that their knee angle was at 90 degrees from the thighs, their torso recline and neck angles were at zero degrees from the vertical axis, their arms as vertical as the manikin adjustment allowed, and their elbows close to a 90 degree angle from the arm. Although the exact posture of seated subjects was not detailed in Fanger's book [19], Figures 42 to 47 suggest occupants rested their arms on their thighs, which was also the pose adopted by Tanabe et al. [35]. Additional adjustments were made to position the chest slightly forward and the neck slightly back to achieve the desired torso flex angle. Manikin poses used are shown in Figs. 3, 4, and 5.

The manikins were imported into ANSYS Spaceclaim [50] and positioned at the center of a 7-meter radius sphere to remove any impact from the parallel ray assumption used in the ray-tracing method [12,14], whose surface was divided into segments of 15-degree increments. Each manikin was aligned such that its center of mass coincided with the sphere's center, facing α and β of zero. Each section was identified by the spherical angle of its center with respect to the sphere center, with α representing the azimuth and β the altitude.

Manikins Youssef and Adam were modeled in three configurations: *float, stool*, and *chair*, as shown in Figs. 3 and 5, while the Nour manikin was only modeled in the *float* configuration, shown in Fig. 4. The *float* configuration had all three manikins "floating in the air", meaning no chair or supporting object was simulated beneath their thighs.

Seat selection was made to present the breadth of possible shading, from the most minimal amount represented by the *stool*, to the large and highly shading office *chair*. The stool (*stool* configuration) had a height of 0.3817 m for the Youssef manikin and 0.246 m for the Adam manikin.

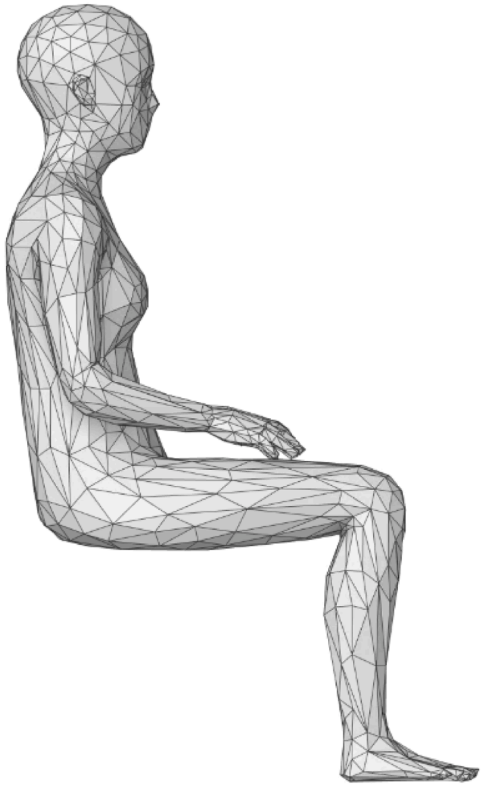

Fig. 4. Nour in the *float* configuration.

It was retrieved from a free 3D model website [51], adjusted to remove structural parts that did not pertain to the radiation calculations (truss, screws), sized and positioned so the bottom of the manikin's feet was level with the base of the stool legs, and the contact area between the manikin and stool seat was proportionally equal between the two manikins.

The Youssef manikin was analyzed seated on an office chair equipped with back and neck support (*chair* configuration), measuring 1.3 m from top to bottom [52]. The backrest, headrest, and seat dimensions were 2650 cm^2, 694 cm^2, and 2135 cm^2, respectively. The Adam manikin was evaluated seated on a school chair (*chair* configuration) from [53], measuring 0.58 m from top to bottom, with backrest and seat dimensions of 401 cm^2 and 751 cm^2, respectively. For all cases, only one-half of the sphere was considered ($0 \leq \alpha \leq 180^{\circ}$ and $-90 \leq \beta \leq 90^{\circ}$), assuming L/R symmetry but not A/P symmetry. All

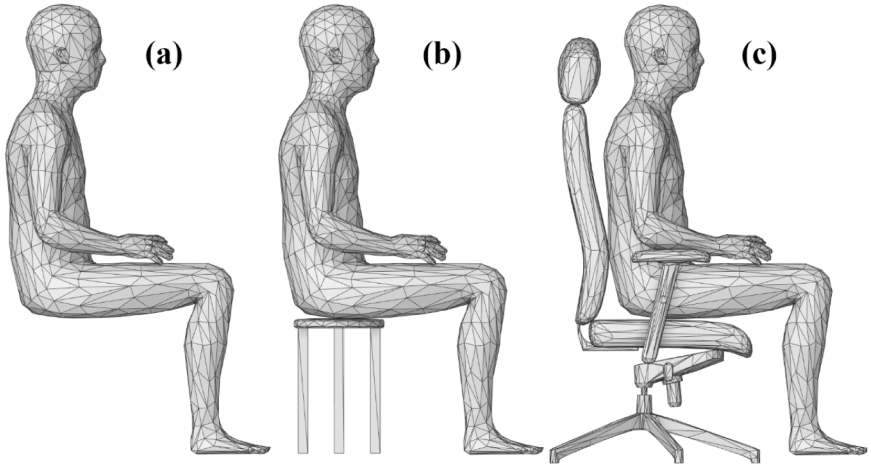

Fig. 3. Youssef in the three seated configurations considered: (a) *float* (b) *stool* (c) *chair*.

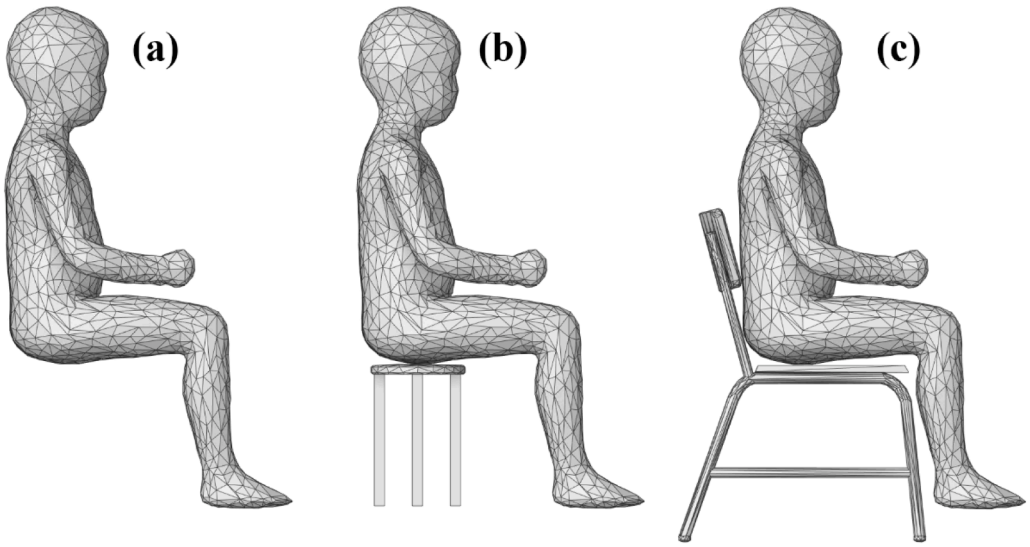

Fig. 5. Adam in the three seated configurations considered: (a) *float* (b) *stool* (c) *chair*.

manikins had their feet areas deselected from radiation calculations as they are assumed to be in contact with the floor.

The manikins were meshed in ANSYS using the patch-independent tetrahedron method, resulting in a total element count ranging from 1.3 to 6.4 million, depending on the configuration. The meshed model was then imported into ANSYS Fluent, where the surface-to-surface radiation model was applied. View factors F_{m-ss} between the manikin m and each selected surface ss were computed using the ray-tracing method, employing a resolution of 100 to minimize aliasing effects. The determined view factors were post processed to minimize the row sum error of the view factor matrix using the least square method [54].

The computed view factor values F_{m-ss} were used to determine f_p for manikin m with respect to each considered sphere surface section ss at an angle (α, β) relative to the manikin's center of volume, following Eqs. (5) and 6. A correction factor f_c was applied to account for the self-radiation effect of the human body, shown in Eq. (4). r_S refers to the sphere radius (7 m), and A_{ss} refers to the sphere section surface area in m^2.

$$F'_{m-ss} = f_c \cdot F_{m-ss} \tag{5}$$

$$f_p = \frac{\pi \times r_s^2 \times F'_{m-ss}}{A_{ss}} \tag{6}$$

A custom code was employed to calculate the view factor F between the occupant and any rectangular surface from the arrays of f_p determined, using Eq. (3) and the summation law.

A theoretical test case from literature was considered to quantify the impact of f_p differences on $\overline{t_r}$. The view factors between an occupant and each surrounding surface was calculated and compared using the f_p data derived from the configurations described above: Youssef and Adam in the three configurations (*float, stool*, and *chair*), as well as the view factors derived from Fanger's data.

4. Results and discussions

4.1. Verification of adult manikin results against literature

The f_p data of the adult manikins Youssef and Nour, in the *float* configuration, are compared to those of Fanger's nude male and female subjects in Figs. 6 and 7, respectively. The f_p values can be found in Tables 1 and 2 in the Appendix. The f_p curves display the same behavior as those found in the Fanger study (Figs. 6 and 7, (a), (b) and (c)).

For the Youssef manikin, the maximum difference found was −27.50 % (Δf_p=−0.0486), with a mean of −5.11 % (Δf_p= −0.0088). For the Nour manikin, the maximum difference found was −26.80 % (Δf_p= −0.0476), with the mean being −6.35 % (Δf_p= −0.0121). The difference is least prominent (<16 % and Δf_p< −0.031) in the higher altitude angles ($\beta = 60°, 75°$, and 90°) where the curves display similar patterns. For shallow altitude angles ($\beta = 0°$ and 15°), the relative difference is lower than 15 % except for the Nour manikin at the middle azimuth angles ($60° \leq \alpha \leq 90°$) where it is higher than 16 %. The highest differences (>16 %) were found for $\beta = 30°$ and 45° and $\alpha \geq 135°$, where the manikins overestimate the values of f_p provided by Fanger. The reduction of the error at higher altitude angles can be attributed to the uniformity of the shape of the manikins and subjects at these angles, where individual differences in body shape and pose are less influential. The magnitude of both absolute and relative differences found is on par with that found in the literature which, as shown in Table 2, are as high as +52 % (Δf_p=0.081).

A regression analysis of the significance of the difference with Fanger's data is conducted and presented in Figs. 6d and 7d, as well as Table 3, where it is compared to the regression performed by Tanabe [35] for each β curve. Overall, the present data slightly overestimates Fanger's results, except at β=15° where Youssef-*float* and Nour-*float* slightly underestimates Fanger's. The Youssef manikin shows a better match with Fanger's men than the Nour manikin with Fanger's women, but the differences found are consistent with those found by Tanabe. Comparing our regression analysis to that of Tanabe, we find that our overall and individual regression coefficients are lower than Tanabe's (overall 1.002), but our coefficients of determination are consistently higher (Tanabe's 0.397 to 0.93, versus our 0.99), indicating our differences from Fanger have smaller variations than the differences between Tanabe and Fanger.

Fig. 8 presents f_p of the Youssef-*float* manikin compared to the numerical results of Tanabe [35]. For all β curves, there is a good match between our results and those of Tanabe, and the regression coefficient found is better than that found with the Fanger data (0.973). Based on this comparison with literature, the proposed method is deemed valid to determine the radiation data of the various numerical manikins and configurations studied.

4.2. Anterior-posterior symmetry in the seated posture and effect of seating

Fig. 9 shows the f_p curves for the Youssef manikin in the three considered configurations: *float, stool*, and *chair*. The tabulated data can be found in Tables 1, 4, and 6 of the Appendix. To analyze the anterior-

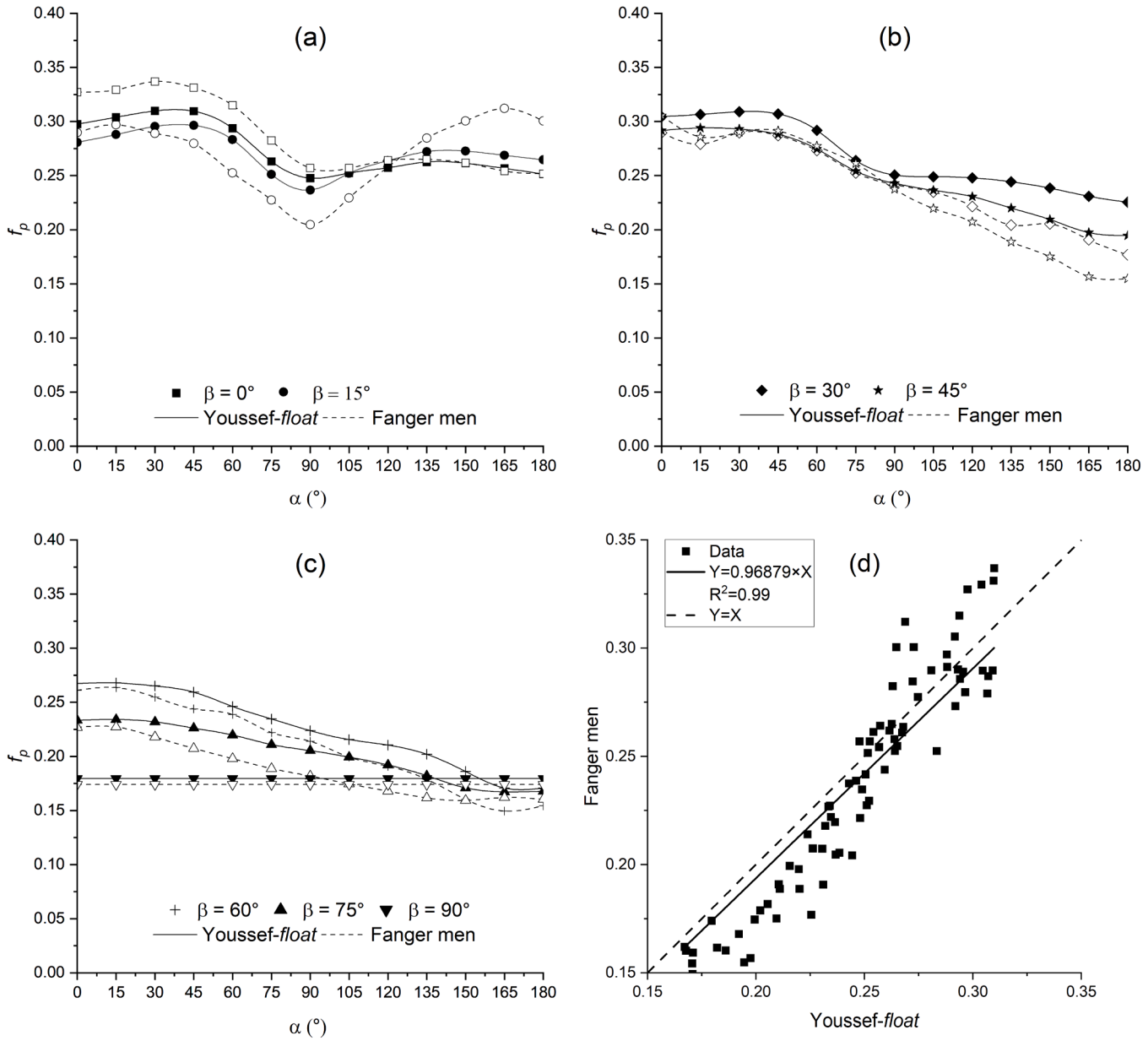

Fig. 6. Comparison of f_p between Youssef-*float* and Fanger's nude male subjects: (a) altitude 0°, 15°; (b) altitude 30°, 45°; (c) altitude 60°, 75°, 90°; (d) correlation of f_p between Youssef-*float* and Fanger's men.

posterior symmetry assumption, each subfigure shows the curve for both the positive and negative altitude as well as the vertical line of symmetry that applies under the A/P symmetry assumption. This assumption implies, for example in Fig. 9a, that the $\beta = -15°$ curve would be symmetrical with the β=15° curve with respect to the vertical symmetry line (highlighted), as deduced from Eq. (4) and Fig. 2b [21].

Looking at the curves of the *float* configuration (dash line for positive β, solid line for the corresponding negative β), the symmetry is present though not perfect. In addition, as Fig. 9f shows, the top-down ($\beta = 90°$) and down-top ($\beta = -90°$) f_p values are comparable when the manikin is floating. This mirrors the findings of past studies [35–38] which simulated manikins in the floating configuration, did not consider negative β and assumed A/P symmetry, which found similar results to those of Fanger. This can lead us to conclude that if the manikin is floating, the A/P symmetry assumption is acceptable.

Analysing Fig. 9 for the *stool* configuration, we find that the symmetry is no longer in place. Comparing the positive β curves of the *stool* configuration (short-dash line) with those of the *float* configuration (dash line), we can see that these configurations are almost identical for positive values of β (difference less than 4 % and 0.006). On the other hand, comparing the negative β curves of the *stool* configuration (dash-dot-dot line) with those of the *float* configuration (solid line), we can see evident difference, where the *stool* configuration has visibly lower values of f_p, due to the blocking effect of the stool. The gap between the two lines is small for the lower values of $\beta = -15°$ and $-30°$ (1 %–12 %, 0.0024–0.0348) and becomes clearly larger as the altitude increases, reaching 28 % and 0.0575 for $\beta = -75°$, and 26 % and 0.0488 for $\beta = -90°$ As a result, the positive (short-dash line) and negative (dash-dot-dot line) β curves for the *stool* configuration do not display symmetry with respect to the vertical symmetry line, and the A/P assumption is not valid.

The *chair* configuration displays even larger differences from both the *float* and *stool* configurations. Comparing the negative β curves of the *chair* configuration (dot line) with those of the *float* configuration (solid line), we can see a very large difference, where the *chair* configuration has visibly lower values of f_p, due to the blocking effect of the chair. The

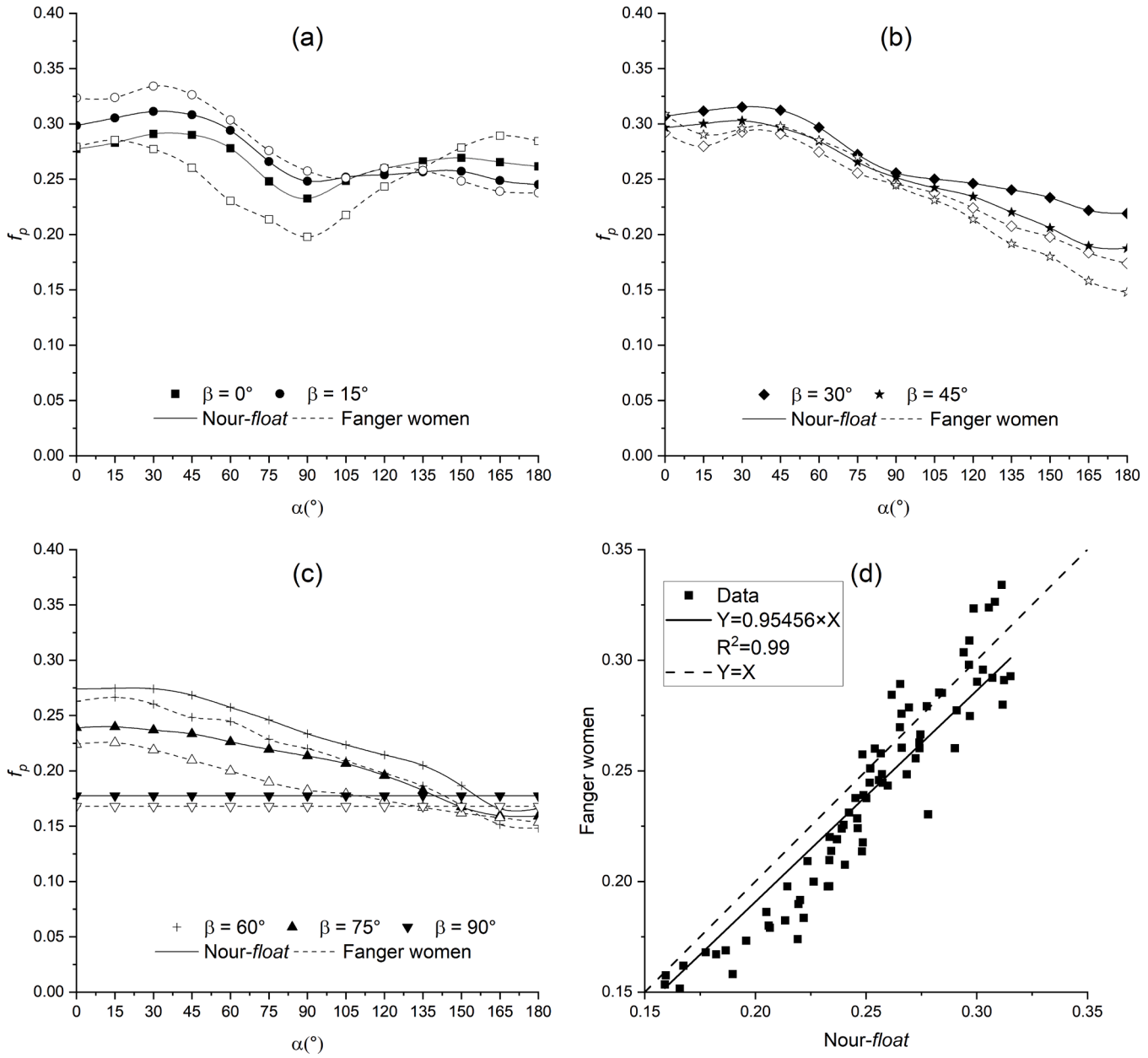

Fig. 7. Comparison of f_p between Nour-*float* and Fanger's nude female subjects: (a) altitude 0°, 15°; (b) altitude 30°, 45°; (c) altitude 60°, 75°, 90°; (d) correlation of f_p between Nour-*float* and Fanger's women.

Table 2
Absolute and relative error between literature and Fanger's experimental results for f_p.

Error	Minimum		Maximum		Mean	
Study	Abs.	Rel.	Abs.	Rel.	Abs.	Rel.
Tanabe et al.	–	−21 %	–	+20 %	–	0 %
La Gennusa et al.	−0.0401	−23 %	0.081	+52 %	−0.001	0 %
Lo Curcio	–	N/S	0.08	45 %	–	N/S
Present: Youssef-*float*	−0.0486	−27.5 %	0.0434	+13.9%	−0.0088	−5.1 %
Present: Nour-*float*	−0.0476	−26.8 %	0.0248	+8.2%	−0.0121	−6.3 %

gap between the two lines is remarkable for both low and high values of β, reaching a maximum of 86 % and 0.235. The largest difference is observed for azimuth angles α >90°, where the blocking effect of the chair back is most influential. Comparing the positive β curves of the *chair* configuration (dash-dot line) with those of the *float* configuration (dash line), it can be observed that for high azimuth (α ≥ 45°) and low altitude (β ≤ 60°), the chair configuration has a lower f_p value than that of the float configuration due to the shading effect of the chair back and seat. For low azimuth (α ≤ 30°), the difference is marginal (<5 %), except for β = +75° where the chair configuration has a higher value than that of the float configuration (average of 10 %). This difference can be explained by A_p being equal between the two configurations for that angle, and A_{eff} being much smaller for the *chair* configuration, making the f_p value of the *chair* configuration larger. Similarly, the A/P symmetry for the *chair* configuration is not valid, as shown in the blue highlight in Fig. 9b

Comparing the chair and stool configurations, the same observations

Table 3
Correlation of f_p with Fanger's results.

Study	β	0°	15°	30°	45°	60°	75°	total
	Metric							
Youssef-*float*	Regression coefficient	1.000	1.049	0.911	0.956	0.940	0.922	0.969
	Coefficient of determination	0.99	0.99	0.99	0.99	0.99	0.99	0.99
Nour-*float*	Regression coefficient	0.957	1.029	0.91	0.96	0.937	0.910	0.955
	Coefficient of determination	0.99	0.99	0.99	0.99	0.99	0.99	0.99
Tanabe (2000)	Regression coefficient	0.99	1.04	0.944	0.979	1.016	1.042	1.002
	Coefficient of determination	0.397	0.739	0.846	0.93	0.964	0.796	0.891

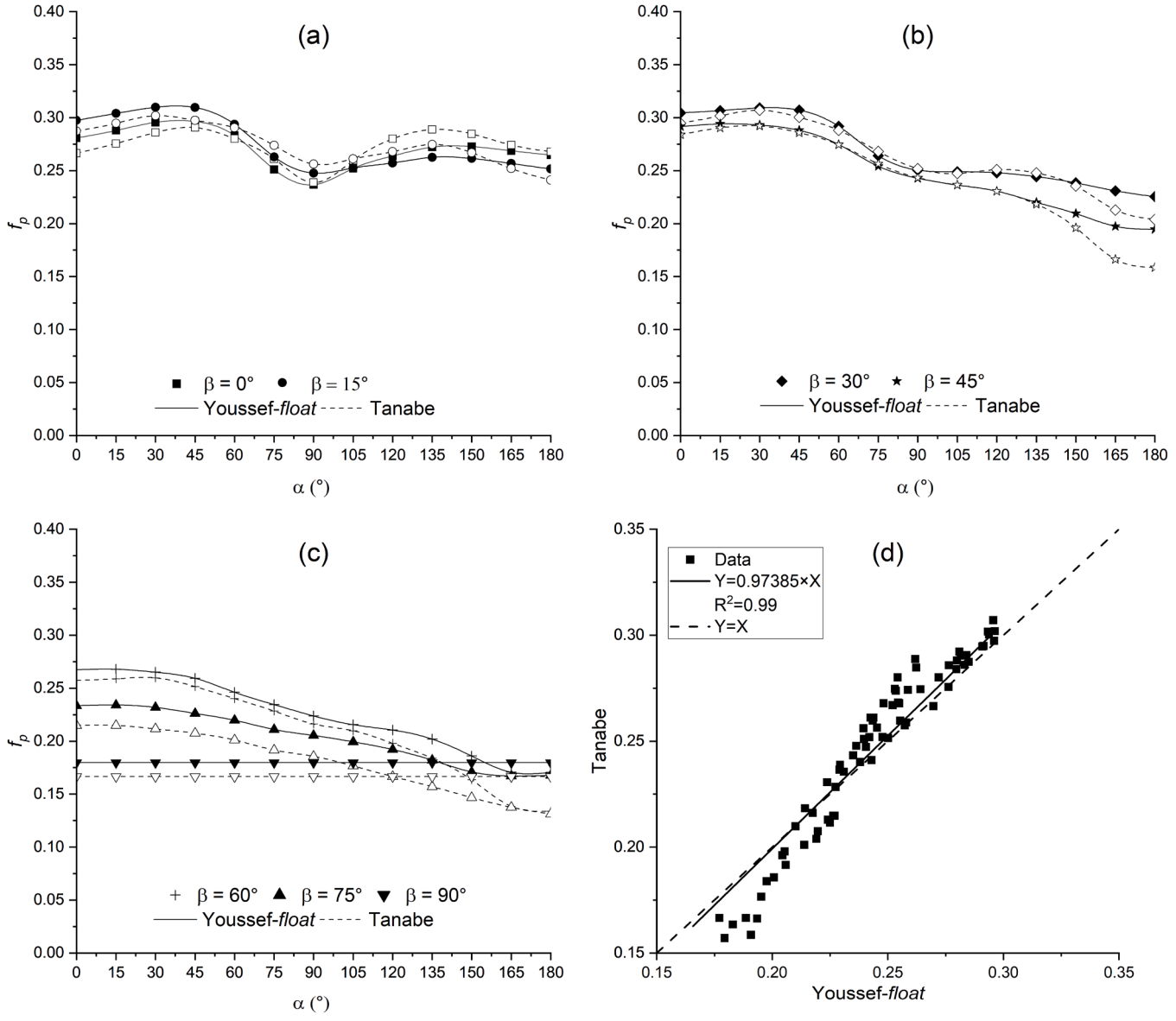

Fig. 8. Comparison of f_p between Youssef-*float* and Tanabe [35]: (a) altitude 0°, 15°; (b) altitude 30°, 45°; (c) altitude 60°, 75°, 90°; (d) correlation of f_p between Youssef-*float* and Tanabe.

can be made, alas to a smaller degree for higher negative altitudes ($\beta \leq -60°$) but comparably for high azimuth angles ($\alpha \geq 90°$) where the shading effect of chair back is noticeable, reaching a difference of 85 % and 0.092 for $\alpha = 180°$ These relative and absolute differences between seat configurations are much larger than the methodological differences with the literature (27 % and 0.048) and can thus be deemed significant.

4.3. Children manikin in different configurations, comparison with adult

The f_p curves of the Adam-*float* manikin are compared to those of the adult Youssef-*float* manikin in Fig. 10. The tabulated data for the Adam manikin in the different configurations are presented in Tables 3, 5, and 7 of the Appendix. As can be seen in Figs. 10a, 10b, and 10c, the curves display a similar shape and there are no distinct patterns like those observed between the adult and child manikins in the standing posture

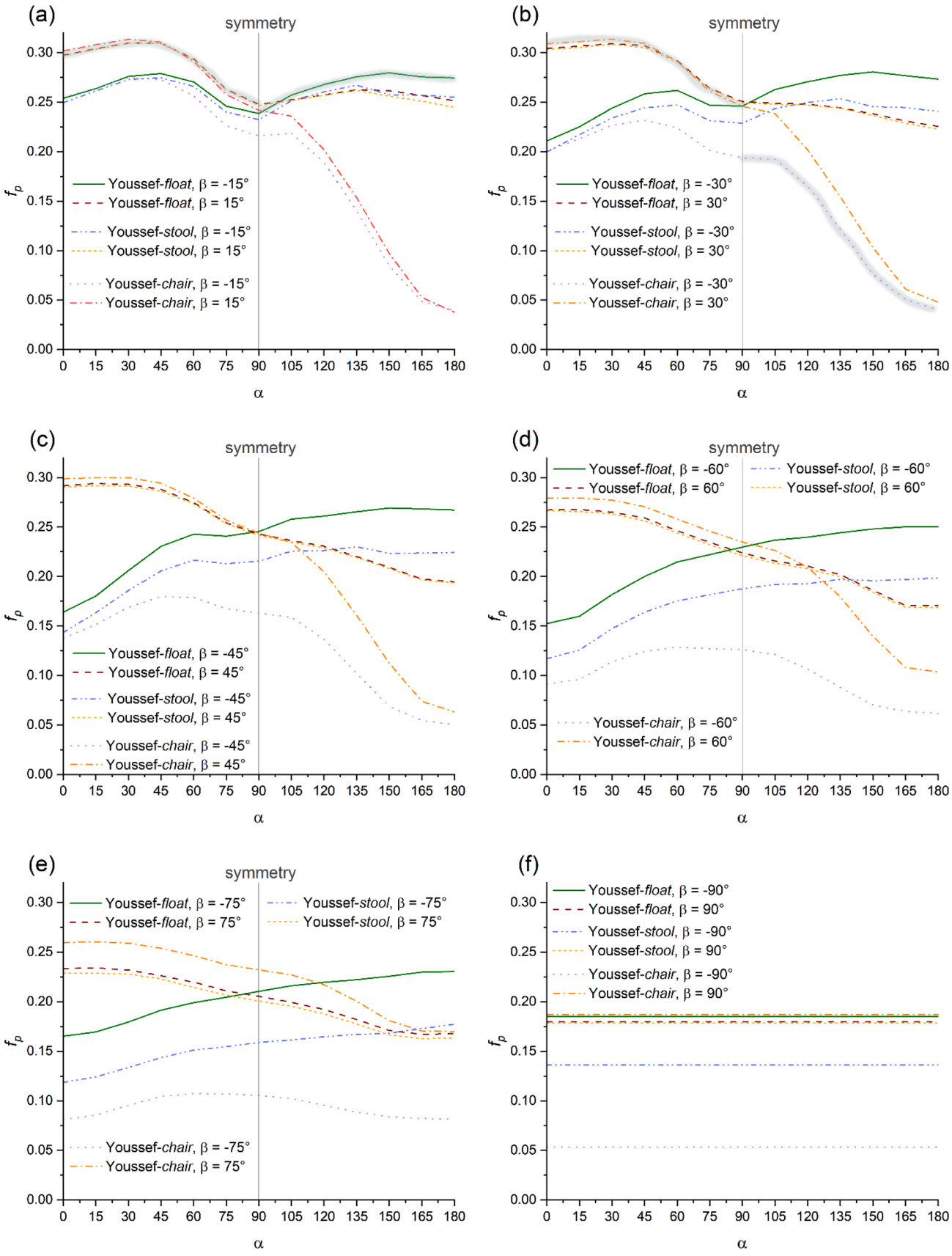

Fig. 9. f_p comparison of the Youssef manikin in different configurations.

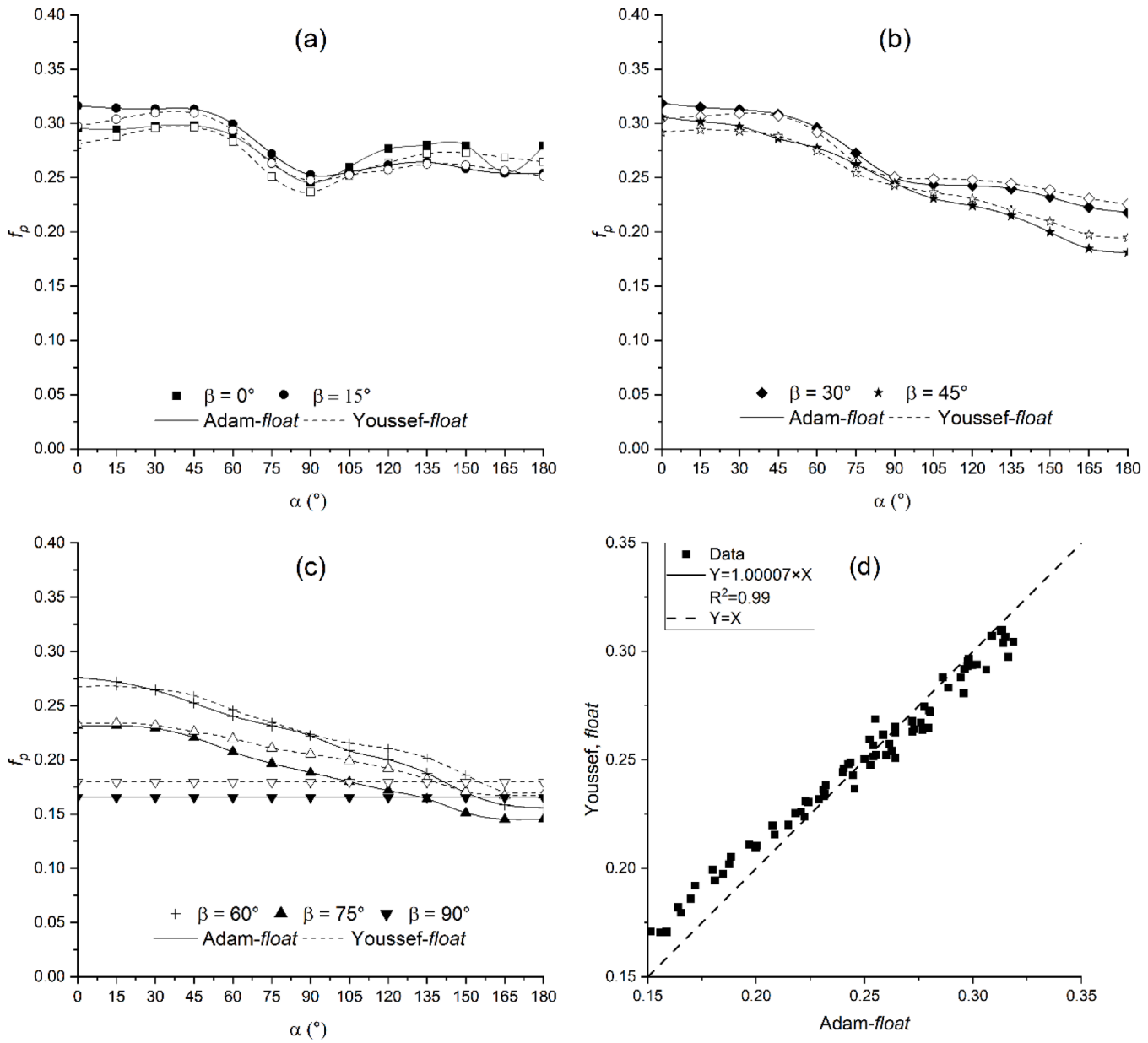

Fig. 10. Comparison of f_p between Adam-*float* and Youssef-*float* (a) altitude 0°, 15°; (b) altitude 30°, 45°; (c) altitude 60°, 75°, 90°; (d) correlation of f_p between Adam-*float* and Youssef-*float*.

[12]. In addition, the regression analysis shown in Fig. 10d shows that the difference between the two sets of data is insignificant. The largest difference observed is 12.63 % and 0.022 for β = −90°, whereas for the positive values of β, the difference is lower than 8 % and 0.018, much smaller than the methodological differences found with the literature (27 % and 0.048). A comparison between the same adult and child manikins in the standing posture resulted in different curve shapes and a consistent difference that reached 22 % and 0.036 [12]. It is likely that the shape and size of the occupant in the seated posture has a smaller effect on their f_p than that observed in the standing posture due to the compact shape of the body in that posture. Though investigations into the seated posture in the literature are scant, comparing the observed population differences in that literature ($\Delta f_p \approx 0.017$ [43]), we can conclude differences between children and adults are insignificant in this posture.

Fig. 11 shows the f_p curves of the Adam manikin in the three configurations: *float, stool*, and *chair*. Similar observations to those made for the Youssef manikin can be made here. The blocking effect of the chair for Adam-*chair* configuration is remarkable (up to 76 % and 0.143) but less than that observed for the Youssef-*chair* configuration (86 % and 0.235). This is because the school chair (shown in Fig. 5c) is significantly smaller compared to the size of the child than the office chair (shown in Fig. 4c) compared to the size of the adult. This results in the school chair having a smaller shading effect, particularly with respect to the back where the Youssef-*chair* manikin has the entire back and head shaded by the chair, whereas the Adam-*chair* manikin's back is only partially shaded.

4.4. Test scenarios

Two theoretical test scenarios are presented to analyze the effect of the differences between adults and children, as well as the effect of seat configuration on the mean radiant temperature. In both scenarios, a room of dimensions 8 × 8 × 4 m, with the occupant seated in the middle, is considered. The adult occupant's center of mass is assumed to be at an altitude of 0.6 m from the floor, based on the recommendations made by

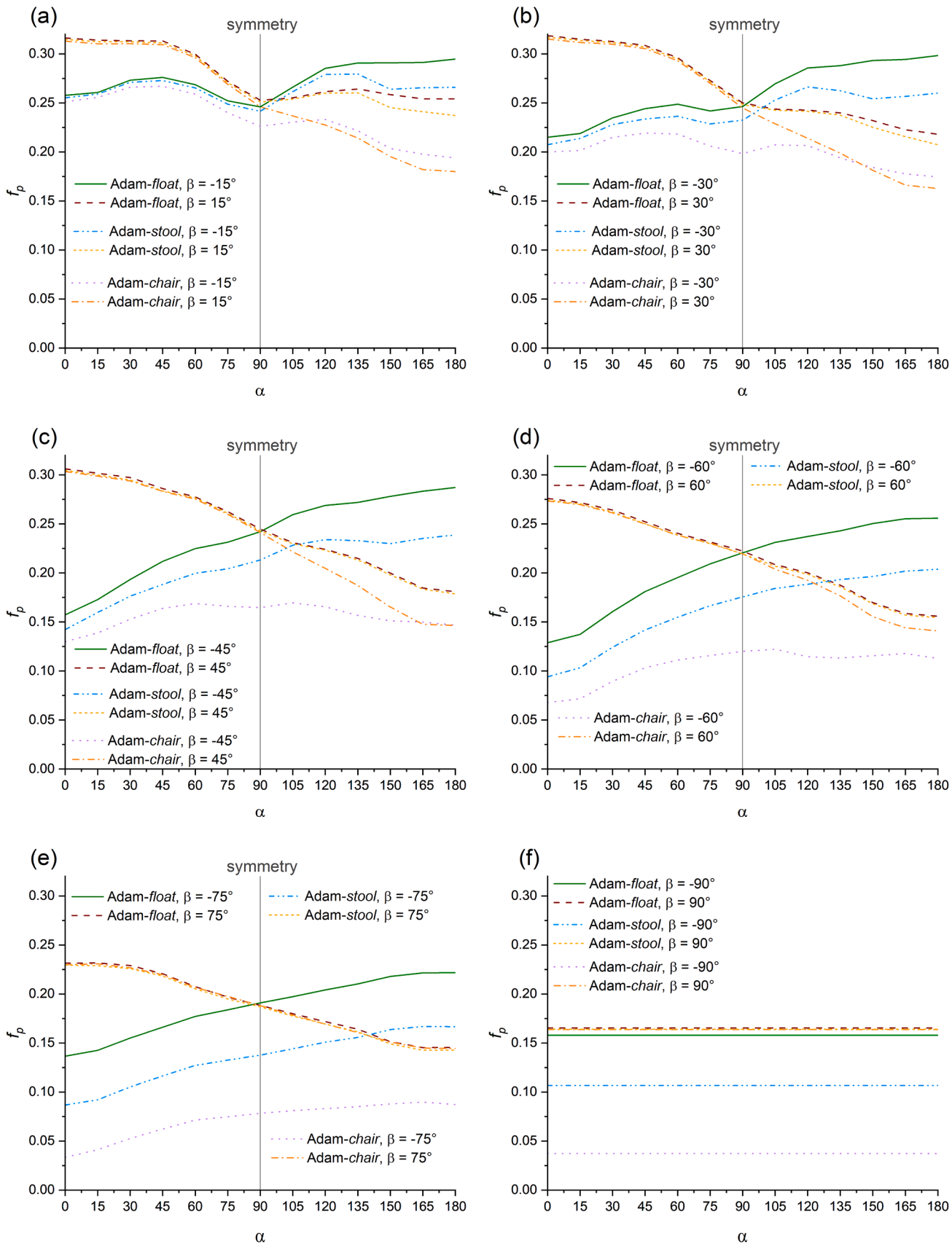

Fig. 11. f_p comparison of the Adam manikin in different configurations.

ASHRAE [16] and Fanger [19] for the seated posture. The child's center of mass is assumed to be at an altitude of 0.24 m based on the abdomen altitude of seated standard 5-year-old [55]. In the first scenario, a "hot floor" with radiant floor heating is used, while in the second, a "cool ceiling" with a chilled ceiling is implemented. The temperature of each surface presented in Table 4 was selected based on the classroom design example from ASHRAE Handbook [22], used by Youssef & D'Avignon [12].

Fig. 12 shows the view factors of the considered occupant with each surface. "Fanger diagrams" refers to the values determined using the view factor diagrams presented by Fanger [19]; "Fanger code" refers to the values calculated using Fanger's f_p arrays and the code developed based on Eq. (3). The values for each manikin configuration were calculated using their corresponding f_p arrays presented previously (tabulated in the Appendix) and the code.

There is a good match between the "Fanger diagrams" and "Fanger code" values (within 2 %) and between the Youssef-*float* and "Fanger code" (within 3 %). Both Youssef and Adam manikins in the *stool* configuration have similar values to those in the *float* configuration for the walls and ceiling (within 3 %) but show a difference of 9 % for the floor. The Adam-*chair* manikin shows a significantly lower F for the rear wall (22 %) and floor (25 %) than the *float* configuration, while the Youssef-*chair* manikin shows an even larger difference for the rear wall (67 %) and the floor (36 %), due to the larger shading of the office chair. Comparing the adult and child manikins, the differences in F are present but less significant than the effect of seating. For the float configuration, Youssef has a lower F than Adam for the floor (by 10 %), and a higher *F* for the ceiling (by 13 %) and rear wall (8 %). This is likely due to the larger altitude (0.6 m) of Youssef than Adam (0.24 m). For the stool configuration, the same variations are found (10 % for the floor, 13 % for the ceiling, and 10 % for the rear wall). For the *chair* configuration, the difference between the two manikins is large, due to the larger shading of the office chair: Youssef's F with the rear wall is half that of Adam's, and his F with the floor is 30 % lower.

Table 5 shows the mean radiant temperature calculated for each configuration using Eq. (1). For both scenarios, the Fanger diagram and code produce the same temperature as both the Youssef-*float* and Adam-*float* manikin. This leads us to conclude that whereas differences of up to 1 °C were reported in similar circumstances in the standing posture between adults and children [12], the differences in the seated posture are negligible. Remarkable differences are found between seat configurations. For Youssef, introducing the stool decreases $\overline{t_r}$ by 0.4 °C in the hot floor scenario and 0.2 °C in the cold ceiling scenario, while introducing the chair decreases it by 2.0 °C and 1.3 °C, respectively. This is due to the chair shading the body from the radiant effect of both the floor and rear wall. For Adam, introducing the stool decreases $\overline{t_r}$ by 0.3 °C in the hot floor scenario and 0.2 °C in the cold ceiling scenario, while the chair decreases it by 1.2 °C and 0.8 °C, respectively.

The effect of a 2 °C difference on occupants' thermal comfort, expressed through the Predicted Mean Vote (PMV), varies according to both environmental conditions and individual characteristics. Several studies have challenged the use of the PMV equation for the prediction of children's thermal comfort as the applicability of several of its terms is limited to adults [55,56]. But the effect of a difference in $\overline{t_r}$ can be propagated to PMV, based on Fanger's [19] PMV sensitivity tables; a 0.5–2 °C shift in $\overline{t_r}$ corresponds to a PMV change of approximately ±0.06 to ±0.24. Alfano et al. [57], who also analyzed the sensitivity of the PMV equation to $\overline{t_r}$ found that a variation of ±0.2 °C resulted in a difference of ±0.16 to ±0.25 in the PMV. These PMV differences (up to 0.2) can result in uncertainty in attribution to a thermal comfort category [23], and can cause failure in predicting real thermal comfort conditions.

Table 4
Temperature of surfaces in Celsius for the test scenarios considered.

Surface	Front	Rear	Left	Right	Ceiling	Floor	Window
Scenario 1: Hot Floor	19.5	20.5	20.5	20.5	18.5	26	18
Scenario 2: Cool Ceiling	24.5	22	23	23	17	21	22

5. Conclusions

The study explored the calculation of f_p for an adult and child manikin in the seated posture. The anterior-posterior symmetry commonly assumed in seated literature was investigated and found to be valid only if the occupants are assumed to be floating in the air. The presence of a seat, even one as nonintrusive as a stool, makes that assumption invalid, and requires the use of negative β values for all realistic scenarios in a seated posture. These findings indicate current view factors F used in the design and evaluation of indoor and outdoor spaces should be revised for the seated posture and dispense of that assumption.

We found seat shading had significant effect on f_p regardless of the seat type considered. The presence of the stool, the most minimalist seat deemed realistic, was found to decrease f_p by up to 28 % (Δf_p=0.0575) for the adult manikin and by up to 36 % (Δf_p=0.055) for the child manikin. The presence of an office chair decreased f_p by up to 86 % (Δf_p=0.235) for the adult manikin due to its large obstruction of radiation, while a school chair decreased the child's f_p by up to 76 % (Δf_p=0.143). The significant differences between chair configurations indicate that chair type may have to be considered in the most severe cases. Generally, it is our recommendation that a minimum chair blocking effect be systematically considered, through the use of appropriate f_p values, when designing radiant systems for spaces where prolonged seating occurs, such as offices and schools.

Differences between the adult and child manikins in the seated posture were found to be minimal (<12 % and <0.022), paling in comparison to differences found between the same standing adult and child manikins (up to 22 % and 0.036) [12].

Two test scenarios were used to investigate the effect of occupant age and chair type on mean radiant temperature. It was found that age effects mean radiant temperature only marginally (less than 0.04 °C), while the presence of a stool, an example of minimalist seating, impacted $\overline{t_r}$ by 0.37 °C for the adult and 0.3 °C for the child. A standard executive office chair resulted in a decrease of 2.0 °C for the adult, while a school chair decreased $\overline{t_r}$ by 1.2 °C for the child. It appears using f_p values in current standards for the calculation of $\overline{t_r}$ may result in a gross overestimation of the effect of radiant surfaces for seated occupants which could impact their thermal comfort in spaces with large radiant surfaces.

This paper clearly establishes the significant effect of the assumptions studied (ie. no seat shading and A/P symmetry) on radiant heat transfer between the body and its environment. In both theoretical test cases considered, correcting these undue assumptions significantly reduced the mean radiant temperature experienced by the occupant from surrounding building surfaces. To confirm their net effect on the occupant's heat balance and thermal comfort, several other important aspects should also be considered such as the relative importance of local discomfort on the back and thighs, clothing insulation increase brought about by the chair presence and type, as well as potential reradiation by the chair to the occupant. Further research is needed to establish the full effect of correcting these radiation assumptions in the seated posture.

CRediT authorship contribution statement

Nour Youssef: Writing – original draft, Validation, Software,

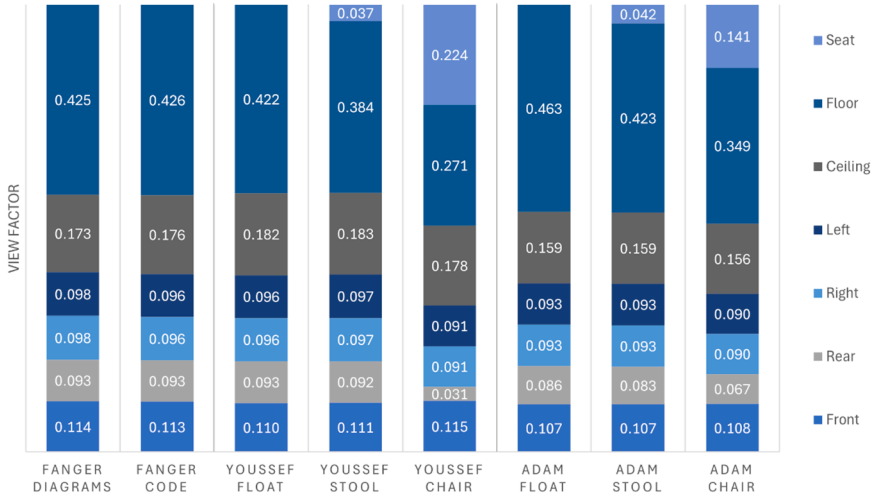

Fig. 12. View factors calculated for each method and configuration.

Table 5
Mean radiant temperature calculated for each method and configuration.

Source	Fanger		Youssef			Adam		
	Diagrams	**Code**	***float***	***stool***	***chair***	***float***	***stool***	***chair***
				Hot Floor				
$\overline{t_r}$ (°C)	23.0	23.1	23.0	22.7	21.1	23.0	22.6	21.8
				Cold Ceiling				
	21.5	21.5	21.5	21.3	20.2	21.5	21.3	20.8

Methodology, Formal analysis. **Katherine D'Avignon:** Writing – review & editing, Supervision, Funding acquisition.

Declaration of competing interest

The authors declare the following financial interests/personal relationships which may be considered as potential competing interests:

Nour Youssef reports financial support was provided by Natural Sciences and Engineering Research Council of Canada. If there are other authors, they declare that they have no known competing financial interests or personal relationships that could have appeared to influence the work reported in this paper.

Acknowledgements

We acknowledge the support of the Natural Sciences and Engineering Research Council of Canada (NSERC), [FRN RGPIN-2020–04986].

Appendix 1 - f_p for the Youssef-*float* manikin

		Youssef-*float*												
	f_p	**β**												
		−90	**−75**	**−60**	**−45**	**−30**	**−15**	**0**	**15**	**30**	**45**	**60**	**75**	**90**
α	**0**	0.185062	0.165161	0.152321	0.164005	0.210764	0.253917	0.280799	0.297537	0.304518	0.291675	0.267318	0.233415	0.179567
	15	0.185062	0.169440	0.159855	0.180218	0.225080	0.263776	0.287941	0.303956	0.306627	0.294024	0.267872	0.234057	0.179567
	30	0.185062	0.179496	0.181791	0.206065	0.243933	0.275985	0.295526	0.309803	0.309120	0.293084	0.265102	0.231918	0.179567
	45	0.185062	0.191478	0.199960	0.230503	0.258504	0.278908	0.296412	0.309516	0.307075	0.288150	0.259342	0.226141	0.179567
	60	0.185062	0.198967	0.214694	0.242722	0.261955	0.270482	0.283291	0.293753	0.291928	0.274678	0.246158	0.219722	0.179567
	75	0.185062	0.204530	0.222117	0.240763	0.246873	0.245950	0.251069	0.263031	0.264064	0.254157	0.234525	0.210949	0.179567
	90	0.185062	0.210521	0.229761	0.245463	0.246170	0.238613	0.236675	0.247726	0.250515	0.242878	0.223779	0.205386	0.179567
	105	0.185062	0.216084	0.236741	0.257995	0.262850	0.257241	0.252121	0.252427	0.248918	0.236377	0.215581	0.199395	0.179567
	120	0.185062	0.219508	0.239732	0.261050	0.270583	0.267903	0.263858	0.257241	0.248023	0.230581	0.210485	0.192120	0.179567
	135	0.185062	0.222289	0.244275	0.265357	0.277101	0.275583	0.272218	0.262572	0.244316	0.220086	0.201954	0.182064	0.179567
	150	0.185062	0.225713	0.248041	0.269274	0.280552	0.279710	0.272716	0.261540	0.238437	0.209433	0.186001	0.170938	0.179567
	165	0.185062	0.229778	0.250257	0.268334	0.276718	0.275526	0.268730	0.256726	0.230959	0.197450	0.170712	0.167086	0.179567
	180	0.185062	0.230634	0.250257	0.267237	0.273331	0.274666	0.264689	0.251567	0.225463	0.194552	0.170601	0.167728	0.179567

Appendix 2 - f_p for the Nour-*float* manikin

		Nour-*float*												
	f_p	β												
		−90	−75	−60	−45	−30	−15	0	15	30	45	60	75	90
α	0	0.182886	0.165933	0.147213	0.156065	0.198187	0.243538	0.277426	0.298561	0.307088	0.296689	0.274033	0.238982	0.177510
	15	0.182886	0.170660	0.158560	0.176435	0.216861	0.253322	0.282985	0.305468	0.311709	0.300150	0.274589	0.239842	0.177510
	30	0.182886	0.179683	0.182923	0.201760	0.235279	0.267251	0.290935	0.311281	0.315302	0.302824	0.274144	0.236834	0.177510
	45	0.182886	0.191071	0.203169	0.225748	0.249910	0.269956	0.290101	0.308173	0.312350	0.296453	0.268359	0.233396	0.177510
	60	0.182886	0.199020	0.217520	0.240612	0.255172	0.263337	0.277981	0.294072	0.296885	0.284341	0.257457	0.226306	0.177510
	75	0.182886	0.206755	0.227198	0.242815	0.246380	0.242847	0.248128	0.265984	0.272435	0.265308	0.245999	0.219431	0.177510
	90	0.182886	0.214704	0.236209	0.249578	0.248755	0.237724	0.232618	0.248315	0.255750	0.251623	0.233539	0.213415	0.177510
	105	0.182886	0.221794	0.243663	0.262949	0.265504	0.256430	0.248517	0.251883	0.250167	0.242264	0.223527	0.206540	0.177510
	120	0.182886	0.226736	0.248335	0.267982	0.274296	0.267826	0.259747	0.253955	0.246188	0.234242	0.214405	0.195797	0.177510
	135	0.182886	0.230388	0.253786	0.273881	0.283344	0.276229	0.266085	0.256660	0.240412	0.220164	0.204949	0.182262	0.177510
	150	0.182886	0.231462	0.255900	0.276319	0.285783	0.280028	0.269365	0.257178	0.233353	0.206007	0.186594	0.167437	0.177510
	165	0.182886	0.233396	0.256345	0.275061	0.281932	0.279165	0.265418	0.248833	0.221802	0.189726	0.165791	0.159488	0.177510
	180	0.182886	0.233826	0.256456	0.274510	0.277761	0.276229	0.261582	0.245207	0.219107	0.187446	0.166013	0.159058	0.177510

Appendix 3 - f_p for the Adam-*float* manikin

		Adam-*float*												
	f_p	β												
		−90	−75	−60	−45	−30	−15	0	15	30	45	60	75	90
α	0	0.157928	0.136596	0.128880	0.157346	0.214962	0.257779	0.295691	0.316200	0.318628	0.306112	0.276012	0.231386	0.165366
	15	0.157928	0.142507	0.137406	0.172880	0.218872	0.260606	0.294435	0.313994	0.314907	0.301707	0.271858	0.231597	0.165366
	30	0.157928	0.154963	0.160580	0.193359	0.234699	0.273162	0.297712	0.313372	0.312637	0.297379	0.264097	0.229064	0.165366
	45	0.157928	0.166152	0.181021	0.211752	0.244094	0.275989	0.298040	0.313146	0.308665	0.286019	0.252291	0.220619	0.165366
	60	0.157928	0.177130	0.195341	0.224890	0.248698	0.268524	0.288644	0.299629	0.296116	0.277518	0.240376	0.207530	0.165366
	75	0.157928	0.183885	0.209223	0.231381	0.241824	0.252180	0.264117	0.271974	0.272785	0.262448	0.231632	0.196763	0.165366
	90	0.157928	0.190852	0.220482	0.242124	0.246365	0.245902	0.245381	0.252689	0.249959	0.244751	0.222340	0.188319	0.165366
	105	0.157928	0.197186	0.231194	0.259512	0.269569	0.266036	0.259966	0.255121	0.243527	0.230841	0.208458	0.179874	0.165366
	120	0.157928	0.204152	0.237097	0.268863	0.285712	0.285264	0.276736	0.261511	0.242518	0.224040	0.200150	0.171852	0.165366
	135	0.157928	0.210275	0.243000	0.272031	0.287919	0.290694	0.280232	0.264226	0.239807	0.214843	0.187579	0.164041	0.165366
	150	0.157928	0.217875	0.250433	0.278059	0.293153	0.290863	0.279740	0.258514	0.231988	0.199774	0.169871	0.151374	0.165366
	165	0.157928	0.221464	0.255352	0.283314	0.294288	0.291259	0.254940	0.254046	0.222655	0.184626	0.158612	0.145252	0.165366
	180	0.157928	0.221675	0.255898	0.287101	0.298323	0.294709	0.279522	0.254159	0.218115	0.180994	0.155879	0.145463	0.165366

Appendix 4 - f_p for the Youssef-*stool* manikin

		Youssef-*stool*												
	f_p	β												
		−90	−75	−60	−45	−30	−15	0	15	30	45	60	75	90
α	0	0.136234	0.118687	0.116972	0.143458	0.199617	0.249465	0.279854	0.296630	0.303190	0.290491	0.266427	0.228698	0.178457
	15	0.136234	0.124048	0.125633	0.163476	0.217167	0.261300	0.287567	0.303639	0.305368	0.291747	0.265761	0.228698	0.178457
	30	0.136234	0.133698	0.147396	0.185849	0.234013	0.273019	0.294170	0.309556	0.308378	0.291590	0.263429	0.227840	0.178457
	45	0.136234	0.143562	0.164051	0.205631	0.244262	0.274570	0.296056	0.309499	0.305240	0.286252	0.256323	0.223122	0.178457
	60	0.136234	0.151283	0.175377	0.216543	0.247208	0.265953	0.281851	0.293068	0.290700	0.273456	0.243887	0.214330	0.178457
	75	0.136234	0.154499	0.181706	0.212853	0.231195	0.240044	0.250334	0.262219	0.263093	0.253360	0.232006	0.206610	0.178457
	90	0.136234	0.159003	0.187702	0.215444	0.228697	0.232346	0.236573	0.246708	0.249130	0.241585	0.221013	0.200605	0.178457
	105	0.136234	0.161362	0.192033	0.225649	0.243557	0.251476	0.251444	0.251706	0.247849	0.234755	0.213463	0.195459	0.178457
	120	0.136234	0.164578	0.192699	0.226120	0.249706	0.260381	0.262985	0.256934	0.247144	0.228946	0.207911	0.187739	0.178457
	135	0.136234	0.167152	0.197140	0.230045	0.253485	0.267217	0.271586	0.261932	0.243877	0.219055	0.199694	0.177660	0.178457
	150	0.136234	0.168224	0.195697	0.223451	0.245671	0.257508	0.261986	0.256187	0.236575	0.208065	0.184149	0.166508	0.178457
	165	0.136234	0.172942	0.197029	0.223686	0.244454	0.257106	0.258435	0.251017	0.228633	0.196368	0.169048	0.162648	0.178457
	180	0.136234	0.177231	0.198584	0.224314	0.240739	0.255038	0.253663	0.244927	0.222740	0.193620	0.168715	0.163506	0.178457

Appendix 5 - f_p for the Adam-*stool* manikin

		Adam-*stool*												
	f_p	β												
		−90	−75	−60	−45	−30	−15	0	15	30	45	60	75	90
α	0	0.106619	0.086794	0.094141	0.142294	0.207416	0.255113	0.294277	0.314716	0.316978	0.304645	0.274141	0.229432	0.164128
	15	0.106619	0.092062	0.103304	0.159725	0.213772	0.259064	0.293350	0.312401	0.313705	0.300017	0.270541	0.228800	0.164128
	30	0.106619	0.105125	0.124250	0.176384	0.227931	0.271030	0.296512	0.312401	0.311629	0.294850	0.262141	0.225850	0.164128
	45	0.106619	0.116502	0.141814	0.188339	0.233595	0.272836	0.296894	0.311216	0.307035	0.283667	0.250141	0.218265	0.164128
	60	0.106619	0.127036	0.154905	0.199599	0.236427	0.265329	0.287571	0.298122	0.294952	0.276494	0.238796	0.205202	0.164128
	75	0.106619	0.132514	0.166577	0.204227	0.228497	0.248679	0.262494	0.270635	0.271605	0.260914	0.229959	0.194879	0.164128
	90	0.106619	0.137571	0.175632	0.213173	0.232399	0.241454	0.244558	0.250993	0.248383	0.242790	0.219487	0.186872	0.164128
	105	0.106619	0.144102	0.184250	0.228213	0.253040	0.261548	0.258950	0.253871	0.242531	0.229755	0.206832	0.177391	0.164128
	120	0.106619	0.150844	0.188505	0.234074	0.266256	0.279101	0.275523	0.259911	0.241461	0.223122	0.198759	0.169385	0.164128
	135	0.106619	0.155690	0.193305	0.232917	0.262417	0.279383	0.275360	0.260249	0.237559	0.213327	0.185886	0.161379	0.164128
	150	0.106619	0.163696	0.196359	0.229910	0.254110	0.263918	0.261676	0.245179	0.225099	0.197979	0.168541	0.149159	0.164128
	165	0.106619	0.166857	0.201814	0.235231	0.256690	0.265442	0.260531	0.241059	0.215660	0.183325	0.157086	0.142627	0.164128
	180	0.106619	0.166646	0.203777	0.238779	0.259963	0.265894	0.258841	0.237165	0.207353	0.178698	0.154468	0.142627	0.164128

Appendix 6 - f_p for the Youssef-*chair* manikin

		Youssef-*chair*												
	f_p	β												
		−90	−75	−60	−45	−30	−15	0	15	30	45	60	75	90
α	0	0.053284	0.080958	0.091557	0.137699	0.200653	0.254802	0.285013	0.301810	0.309198	0.298711	0.279393	0.259811	0.186842
	15	0.053284	0.085604	0.096039	0.151381	0.213078	0.264305	0.292280	0.308032	0.311216	0.299948	0.279284	0.260444	0.186842
	30	0.053284	0.095529	0.113642	0.169005	0.226575	0.274940	0.298618	0.313576	0.313676	0.299870	0.277207	0.259178	0.186842
	45	0.053284	0.104397	0.124248	0.179672	0.231621	0.272734	0.297525	0.310691	0.309513	0.294459	0.270537	0.253899	0.186842
	60	0.053284	0.107142	0.128621	0.178899	0.224052	0.256329	0.278566	0.291288	0.291097	0.279154	0.257964	0.246508	0.186842
	75	0.053284	0.106931	0.127090	0.167381	0.201032	0.226179	0.243871	0.257687	0.260886	0.257047	0.245718	0.237428	0.186842
	90	0.053284	0.105453	0.125997	0.163053	0.193778	0.215997	0.229829	0.241678	0.245875	0.243829	0.234894	0.232149	0.186842
	105	0.053284	0.102286	0.121077	0.158801	0.192139	0.218542	0.230430	0.235909	0.238496	0.234399	0.226257	0.227081	0.186842
	120	0.053284	0.095529	0.106535	0.136694	0.165397	0.189184	0.201472	0.201912	0.201978	0.204794	0.209529	0.217157	0.186842
	135	0.053284	0.088771	0.087949	0.102142	0.121878	0.140253	0.153336	0.153320	0.154359	0.160734	0.179571	0.200475	0.186842
	150	0.053284	0.083915	0.070236	0.068749	0.076152	0.084817	0.094600	0.097205	0.103272	0.112422	0.139664	0.180837	0.186842
	165	0.053284	0.082225	0.063786	0.054526	0.050545	0.048671	0.050125	0.052687	0.061078	0.073773	0.108066	0.170490	0.186842
	180	0.053284	0.081381	0.061490	0.050352	0.040390	0.039620	0.038378	0.037810	0.047896	0.063106	0.103583	0.169857	0.186842

Appendix 7 - f_p for the Adam-*chair* manikin

		Adam-*chair*												
	f_p	β												
		−90	−75	−60	−45	−30	−15	0	15	30	45	60	75	90
α	0	0.037253	0.033383	0.067773	0.130005	0.199937	0.251198	0.292172	0.312950	0.315127	0.303511	0.273403	0.229863	0.163750
	15	0.037253	0.041108	0.071665	0.138872	0.201559	0.255561	0.291470	0.310209	0.311697	0.298695	0.269727	0.230698	0.163750
	30	0.037253	0.052592	0.089504	0.152783	0.214842	0.266021	0.295036	0.310433	0.309826	0.293880	0.261187	0.226731	0.163750
	45	0.037253	0.062197	0.103234	0.163866	0.219146	0.267027	0.294550	0.309426	0.305335	0.283103	0.249943	0.219632	0.163750
	60	0.037253	0.071384	0.111126	0.168834	0.218273	0.258973	0.286067	0.296058	0.293049	0.275306	0.238267	0.206686	0.163750
	75	0.037253	0.074725	0.115775	0.166006	0.205987	0.240011	0.261269	0.269041	0.270036	0.259867	0.230483	0.197499	0.163750
	90	0.037253	0.078275	0.119992	0.164706	0.198378	0.226083	0.237713	0.245996	0.244716	0.241293	0.219455	0.188103	0.163750
	105	0.037253	0.080989	0.122154	0.169598	0.207171	0.230446	0.239172	0.236655	0.228688	0.221573	0.203779	0.178498	0.163750
	120	0.037253	0.083077	0.114586	0.165471	0.206548	0.233019	0.238794	0.227537	0.213907	0.204681	0.192643	0.169311	0.163750
	135	0.037253	0.085165	0.113181	0.156681	0.193950	0.221608	0.225341	0.214225	0.198752	0.187254	0.176643	0.160750	0.163750
	150	0.037253	0.087879	0.115559	0.151177	0.184096	0.203485	0.208160	0.195151	0.181290	0.165241	0.155453	0.150937	0.163750
	165	0.037253	0.089759	0.117829	0.149878	0.177610	0.197612	0.200002	0.181950	0.166072	0.147585	0.143993	0.144882	0.163750
	180	0.037253	0.087253	0.112748	0.146744	0.174492	0.193920	0.194329	0.179936	0.162642	0.146515	0.140965	0.144255	0.163750

Data availability

Data will be made available on request.

References

[1] N. Kántor, J. Unger, The most problematic variable in the course of human-biometeorological comfort assessment-the mean radiant temperature, Cent. Eur. J. Geosci. 3 (2011) 90–100.

[2] A.D. Flouris, P.C. Dinas, L.G. Ioannou, et al., Workers' health and productivity under occupational heat strain: a systematic review and meta-analysis, Lancet Planet. Health 2 (2018) e521–e531.

[3] P. Habibi, J. Razmjouei, A. Moradi, et al., Climate change and heat stress resilient outdoor workers: findings from systematic literature review, BMC. Public Health 24 (2024) 1711.

[4] Y. Fan, K.A. McColl, Widespread outdoor exposure to uncompensable heat stress with warming, Commun. Earth. Environ. 5 (2024), https://doi.org/10.1038/S43247-024-01930-6. Epub ahead of print 1 December.

[5] M.L. Imhoff, P. Zhang, R.E. Wolfe, et al., Remote sensing of the urban heat island effect across biomes in the continental USA, Remote Sens. Environ. 114 (2010) 504–513.

[6] G. Liu, K. Nagano, M. Ye, et al., Optimization of a radiant heating system in a net zero energy house (nZEH) to maintain a comfortable indoor environment while minimizing energy consumption, Energy Build. 328 (2025) 115208.

[7] S.M. Hooshmand, H. Zhang, H. Javidanfar, et al., A review of local radiant heating systems and their effects on thermal comfort and sensation, Energy Build. 296 (2023) 113331.

[8] Natural Resources Canada, Fact sheet: reducing electric heating costs with radiant floors. https://publications.gc.ca/collections/collection_2025/rncan-nrcan/M154-170-2024-eng.pdf, 2024 accessed 20 July 2025.

[9] R. Hu, J.L. Niu, A review of the application of radiant cooling & heating systems in Mainland China, Energy Build. 52 (2012) 11–19.

[10] K.N. Rhee, K.W. Kim, A 50 year review of basic and applied research in radiant heating and cooling systems for the built environment, Build. Environ. 91 (2015) 166–190.

[11] United States Environmental Protection Agency, Improving your indoor environment | US EPA, *Improving Your Indoor Environment*, https://www.epa.gov/indoor-air-quality-iaq/improving-your-indoor-environment#text, 2025. accessed 20 July 2025.

[12] N. Youssef, K. D'Avignon, Considering child-specific view factors in human thermal balance, Sci. Techn. Built Env. 31 (8) (2025) 889–904, https://doi.org/10.1080/23744731.2025.2518734.

[13] K. Rykaczewski, L. Bartels, D.M. Martinez, et al., Human body radiation area factors for diverse adult population, Int. J. Biometeorol. 66 (2022) 2357–2367.

[14] T. Horikoshi, T.Y. Tsuchikawa Kobayashi, K. Miwa Kurazumi, E.Y. Hirayama, The effective radiation area and angle factor between man and a rectangular plane near him, *ASHRAE Trans.* ASHRAE Transact. (1990) 60–66.

[15] Y. Kurazumi, T. Tsuchikawa, N. Matsubara, et al., Effect of posture on the heat transfer areas of the human body, Build. Environ. 43 (2008) 1555–1565.

[16] ASHRAE-55, Thermal environmental conditions for human occupancy, ANSI/ASHRAE Standard - 55 7 (2017) 1–14.

[17] F.R. d'Ambrosio Alfano, M. Dell'isola, G. Ficco, et al., On the measurement of the mean radiant temperature by means of globes: an experimental investigation under black enclosure conditions, Build. Environ. 193 (2021) 107655.

[18] F.R. d'Ambrosio Alfano, D. Pepe, G. Riccio, et al., On the effects of the mean radiant temperature evaluation in the assessment of thermal comfort by dynamic energy simulation tools, Build. Environ. 236 (2023) 110254.

[19] P.O. Fanger, Thermal comfort. Analysis and Applications in Environmental Engineering, Danish Technical Press., Copenhagen, 1970. https://www.cabdirect.org/cabdirect/abstract/19722700268.

[20] E. Arens, T. Hoyt, X. Zhou, et al., Modeling the comfort effects of short-wave solar radiation indoors, Build. Environ. 88 (2015) 3–9.

[21] F. Tartarini, S. Schiavon, T. Cheung, et al., CBE Thermal Comfort Tool: online tool for thermal comfort calculations and visualizations, SoftwareX. 12 (2020), https://doi.org/10.1016/j.softx.2020.100563. Epub ahead of print 1 July.

[22] ASHRAE. 2017 ASHRAE handbook. *Fundamentals.* Atlanta, GA : ASHRAE, [2017], 2017.

[23] Standardization IO for ISO 7730: moderate, Thermal environments-determination of the PMV and PPD indices and specification of the conditions for thermal comfort, 2005.

[24] D. Hope, T.C. Bates, D. Dykiert, et al., Bodily symmetry increases across human childhood, Early Hum. Dev. 89 (2013) 531–535.

[25] G. Rizzo, G. Franzitta, G. Cannistraro, Algorithms for the calculation of the mean projected area factors of seated and standing persons, Energy Build. 17 (1991) 221–230.

[26] G. Cannistraro, G. Franzitta, C. Giaconia, et al., Algorithms for the calculation of the view factors between human body and rectangular surfaces in parallelepiped environments, Energy Build. 19 (1992) 51–60.

[27] L.N. Kalisperis, M. Steinman, L.H. Summers, Angle factor graphs for a person to inclined surfaces, ASHRAe Trans. 97 (1991) 809–839. Indianapolis.

[28] N. Youssef, K. D'Avignon, Investigation into the pertinence of using child-specific radiation data for thermal comfort calculations, ASHRAE Trans. 2 (2023) 81–92, https://doi.org/10.1080/23744731.2025.2518734.

[29] M. La Gennusa, A. Nucara, M. Pietrafesa, et al., A model for managing and evaluating solar radiation for indoor thermal comfort, Solar Energy 81 (2007) 594–606.

[30] M. La Gennusa, A. Nucara, M. Pietrafesa, et al., Angle factors and projected area factors for comfort analysis of subjects in complex confined enclosures: analytical relations and experimental results, Indoor and Built Environ. 17 (2008) 346–360.

[31] F. Calvino, M. La Gennusa, G. Rizzo, et al., Measurements of projected areas of seated and standing people of southern Italy based on a statistical analysis, Appl. Ergon. 40 (2009) 239–250.

[32] F. Calvino, Gennusa M La, A. Nucara, et al., Evaluating human body area factors from digital images: a measurement tool for a better evaluation of the ergonomics of working places, Occupational Ergon. 5 (2005) 173–185.

[33] F.P. Lo Curcio, *Scambi Termici Tra Corpo Umano Ed Ambiente Indoor: Verifi Ca Della Validità Degli Algoritmi Per Il Calcolo Del Fattore Di Area Proiettata*, University of Palermo (in Italian), 2009. Degree Thesis.

[34] Nucara A., Pietrafesa M., Rizzo G., et al. Handbook of anthropometry: physical measures of Human form in health and disease. Epub ahead of print 2012. DOI: 10.1007/978-1-4419-1788-1_4.

[35] S. Tanabe, C. Narita, Y. Ozeki, et al., Effective radiation area of human body calculated by a numerical simulation, Energy Build. 32 (2000) 205–215.

[36] K. Kubaha, D. Fiala, J. Toftum, et al., Human projected area factors for detailed direct and diffuse solar radiation analysis, Int. J. Biometeorol. 49 (2004) 113–129.

[37] M. Havgaard Vorre, R. Lund Jensen, J. Le Dréau, Radiation exchange between persons and surfaces for building energy simulations, Energy Build. 101 (2015) 110–121.

[38] M. Manabe, H. Yamazaki, K. Sakai, Shape factor simulation for the thermal radiation environment of the human body and the VRML visualization, Build. Environ. 39 (2004) 927–937.

[39] Z. Li, X. Feng, X. Fan, et al., Effect of direct solar projected area factor on outdoor thermal comfort evaluation: a case study in Shanghai, China, Urban. Clim. 41 (2022) 101033.

[40] Y. Zeng, Y. Liang, M. Luo, et al., Calculating the local and overall view factors of a multi-segment human model, Energy Build. (2024) 114967.

[41] S.C. Francisco, A.M. Raimundo, A.M. Gaspar, et al., Numerical evaluation of radiative heat exchanges between human beings and cooling radiant systems, in: Proceedings of 7th Windsor Conference: The changing context of comfort in an unpredictable world, 2012, pp. 1–12. *Cumberland Lodge, Windsor, UK12-15 April*.

[42] ISO 7726, International Organization for Standardization: ergonomics of the thermal environment — Instruments for measuring physical quantities, ISO Standard 1998 (1998) 1–56.

[43] S. Park, S.E. Tuller, Human body area factors for radiation exchange analysis: standing and walking postures, Article in Int. J. Biometeorol. (2011), https://doi.org/10.1007/s00484-010-0385-2. Epub ahead of print.

[44] TheGlobalEconomy.com. (2025), Percent children by country, around the world. https://www.theglobaleconomy.com/rankings/percent_children/#:~:text=Population%20ages%200%2D14%2C%20percent,Download%20data%20from%20our%20database, https://www.theglobaleconomy.com/rankings/percent_children/ (accessed 10 September 2025).

[45] A.R. Frisancho, Anthropometric standards: an Interactive Nutritional Reference of Body Size and Body Composition For Children and Adults, University of Michigan Press, 2008.

[46] M. La Gennusa, A. Nucara, G. Rizzo, et al., The calculation of the mean radiant temperature of a subject exposed to the solar radiation - A generalised algorithm, Build. Environ. 40 (2005) 367–375.

[47] UMTRI BioHuman: 3d Human Shapes, University of Michigan Transportation Research Institute, 2020. http://humanshape.org/. accessed 6 February 2024.

[48] A.M. Fredriks, S. Van Buuren, W.J.M. Van Heel, et al., Nationwide age references for sitting height, leg length, and sitting height/height ratio, and their diagnostic value for disproportionate growth disorders, Arch. Dis. Child 90 (2005) 807–812.

[49] Blender 4.4 manual, (2025), https://docs.blender.org/manual/en/latest/index.html (accessed 9 June 2025).

[50] ANSYS, ANSYS FLUENT 12.0 user's guide - 13.3.3 setting up the S2S model. https://www.afs.enea.it/project/neptunius/docs/fluent/html/ug/node475.htm#sec-s2s-viewfactorsmethod, 2010 accessed 6 February 2024.

[51] free3d.com user ksalk3d, Wood Stool 3D Model, https://free3d.com/3d-model/wood-stool-303532.html, 2019. accessed 12 January 2025.

[52] free3d.com user printable_models, Office Chair v1 3D Model, https://free3d.com/3d-model/office-chair-v1–160271.html, 2019. accessed 12 January 2025.

[53] cgtrader.com user Rafor. (2025), Chair and school desk free low-poly 3D model.

[54] M.E. Larsen, J.R. Howell, Least-squares smoothing of direct-exchange areas in zonal analysis, J. Heat. Transfer. 108 (1986) 239–242.

[55] N. Youssef, K. D'Avignon, Evaluating thermal comfort of children: A perspective on commonly used methods, ASHRAE Trans. (2021) 569–579.

[56] S. Gao, W. Oh, C. Lin, et al., A review of thermal comfort of 4- to 14-year-old children via field experiments: experimental designs and methods, Energy Build. 322 (2024) 114687.

[57] Romana F Alfano d'Ambrosio, E. Ianniello, et al., PMV-PPD and acceptability in naturally ventilated schools, Build. Environ. 67 (2013) 129–137.